

Muh-Cherng Wu · Jian-Ren Chen · Jung-Hong Chuang

## An A-trimmed skeleton for modeling the global shape of polygons

Received: 16 February 2004 / Accepted: 15 June 2004 / Published online: 2 March 2005  
© Springer-Verlag London Limited 2005

**Abstract** A skeleton is a global shape descriptor that aims to characterize the general appearance of an object to facilitate object classification. Various ways for defining the skeleton of a polygon have been proposed in the literature. Yet, in some cases, these previously proposed skeletons may not intuitively resemble the original polygons and cannot be a good shape descriptor. This research proposes a new definition of skeletons for modeling polygons. The proposed skeleton is termed the area-trimmed (A-trimmed) skeleton. In modeling the global shape of polygons, the A-trimmed skeleton performs much better than other skeletons proposed in the literature. The A-trimmed skeleton can be applied in group technology and facilitate tasks such as punched-part design and fixture design.

**Keywords** Global shape descriptor · Group technology · Medial axis · Polygon · Skeleton

### 1 Introduction

A skeleton is a global shape descriptor intended to concisely model the general appearance of a 2D/3D object. One application of skeletons is group technology (GT), in which objects are automatically clustered into groups based on the similarity of their skeletons. Such an application implies that the skeletons should resemble the global shape of the modeled objects as closely as possible. The applications of GT based on skeletons include part design [1, 2] and modular fixture design [3].

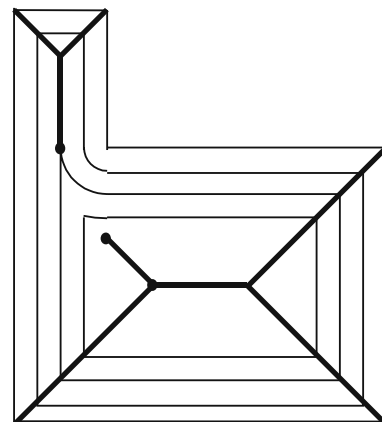
The concept of a skeleton was first proposed by Blum [4] in 1967. According to Blum's definition, the skeleton of a 2D object

is the locus of the centers of all of the maximally inscribed circles of the object. The skeleton so defined is called the medial axis transform (MAT). The MAT can be derived by a "grass-firing" method [5]. Imagining a 2D object as a patch of grass, we simultaneously set the border of the patch on fire. The fire moves like a wave until the grassland is burned. The MAT of the object is the set of points where two or more wavefronts meet together (Fig. 1). Some other algorithms for deriving the MAT can be referred to in [6–8].

The MAT representation has two drawbacks. First, the skeleton may be more complex than its original polygon. As shown in Fig 1, the L-shaped polygon comprises only six line segments, yet its skeleton involves nine segments and one of them is a curved segment. Second, two polygons with similar global shapes may produce dissimilar skeletons. As shown in Fig. 2, the three polygons are similar in shape and only vary by the position of the protrusion on the block; yet their MATs differ significantly in the topology and the number of skeleton links. These phenomena can cause inappropriate results in object clustering applications.

The fire propagation model in [5] is wave-based and may create curved segments on the MAT of a polygon. To overcome the drawbacks, Bookstein [9] proposed an offset-based fire propaga-

**Fig. 1.** MAT of an L-shaped object



M.-C. Wu (✉) · J.-R. Chen  
Department of Industrial Engineering and Management,  
National Chiao Tung University,  
Hsin-Chu, Taiwan, ROC  
E-mail: mcwu@cc.nctu.edu.tw  
Fax: +886-35-720610

J.-H. Chuang  
Department of Computer Science and Information Engineering,  
National Chiao Tung University,  
Hsin-Chu, Taiwan, ROC

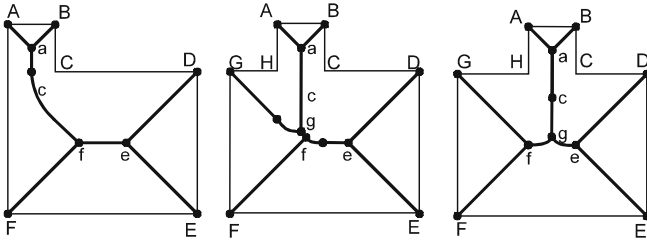


Fig. 2. MAT is sensitive to the variation of geometric features in a polygon

tion mode, which does not produce curved segments, yet might produce a null skeleton (an empty set) for some polygons [10].

To overcome the null skeleton problem, Wu and Chen [10] proposed a ray-based fire propagation model. The associated skeleton is termed the ray-based complete skeleton (or simply the ray-based skeleton). The ray-based skeleton in general looks more complex than the original polygon. For example, the ray-based skeleton of a six-edge polygon involves nine line segments (Fig. 3b). A method is therefore proposed for trimming the ray-based skeleton [10]. The skeleton links to be trimmed away are like leaves on a tree. We therefore name the process as “leaf-trimming”, and the resulting skeleton (Fig. 3c) is called the leaf-trimmed skeleton.

The leaf-trimmed skeleton may not quite resemble the original polygon (Fig. 3a). Wu, Chen, and Jen [11] therefore proposed another trimming method for removing more skeleton links. The resulting skeleton is called the graft-trimmed skeleton (Fig. 3d), which appears to be a better global shape descriptor than the leaf-trimmed skeleton. However, the graft-trimming method appears only applicable to rectilinear polygons (polygons where each corner measures 90°).

This paper presents a new trimming method that can effectively prune the ray-based skeletons for both rectilinear and

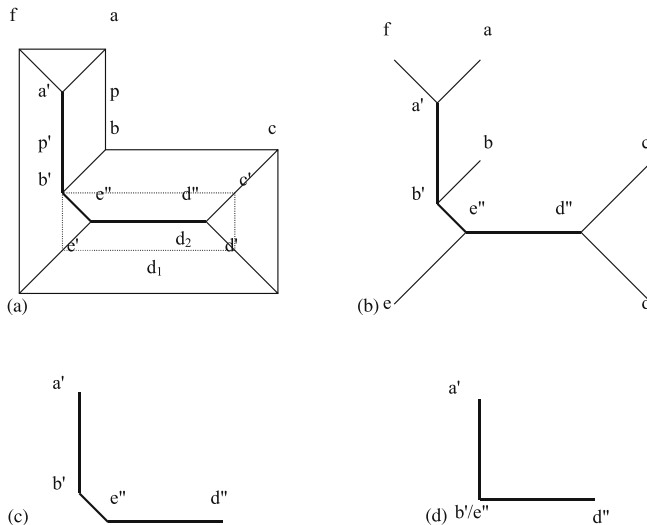


Fig. 3a–d. The ray-based skeleton of an L-shaped polygon. a The fire propagation model. b The ray-based skeleton. c The leaf-trimmed skeleton. d The graft-trimmed skeleton

non-rectilinear polygons. The new trimming method is called area-based trimming (A-trimming). After testing many examples, the A-trimming skeleton appears to be a better global shape descriptor of 2D polygons than those proposed in the literature.

The remainder of this paper is organized as follows: Sect. 2 reviews the algorithm for deriving the ray-based skeleton proposed in [10]. Section 3 presents the A-trimming method. Section 4 analyzes the properties of the A-trimmed skeleton and other skeletons proposed in the literature; some of the tested examples are also illustrated. Concluding remarks are given in Sect. 5.

## 2 Ray-based fire propagation model

The ray-based fire propagation model and the skeletonization algorithm, proposed in [10], are briefly described here. The leaf-trimming method [10] and the graft-trimming method [11] are also illustrated.

### 2.1 Fire propagation model

The ray-based fire propagation model of a polygon  $P$  is based on the following four rules.

- Rule 1: edge-moving. Any edge on polygon  $P$  should propagate along its inward normal at a uniform speed.
- Rule 2: vertex moving. Any corner vertex on polygon  $P$  should move along the bisector of its angle.
- Rule 3: interior point moving. Any interior point ( $X$ ) on an edge ( $\overline{V_1V_2}$ ) should move along a path that is the linear interpolation of the moving paths of  $V_1$  and  $V_2$ .
- Rule 4: shrinkage cycle. When two moving edges that are originally non-neighboring meet, it is called the completion of a shrinkage cycle. The resulting polygon becomes an area joined by dangling edges. A dangling edge is one where one of its end-points does not join any other edge. Dangling edges cannot be shrunk further and should be removed, and the remaining area should be shrunk further until an empty set is obtained.

The ray-based complete skeleton of a polygon is the point set given by the intersections of any two moving edges in each shrinkage cycle.

The ray-based fire propagation model is illustrated by referring to the L-shaped polygon in Fig. 3a. According to rule 1, edge  $\overline{ab}$  moves toward  $\overline{a'b'}$  and line  $\overline{ab}$  is parallel to line  $\overline{a'b'}$ . According to rule 2, the moving trace of vertex  $a$  is  $\overline{aa'}$ , which is on the angle bisector. According to rule 3, for an interior point  $p$  on edge  $\overline{ab}$  ( $p = \lambda a + \gamma b$ ), its moving trace is  $\overline{pp'} = \lambda \overline{aa'} + \gamma \overline{bb'}$ .

According to rule 4, when the two non-neighboring edges  $\overline{ab}$  and  $\overline{ef}$  meet at edge  $\overline{a'b'}$ , the polygon shrinks to an area ( $b'c'd'e'$ ) joined by a dangling edge  $\overline{a'b'}$ . Removing the dangling edge, the remaining area requires further shrinkage. The resulting ray-based complete skeleton involves nine segments where each one is the intersection of two or more moving edges (Fig. 3b).

2.2 Critical shrinkage distance

At the end of a shrinkage cycle (Fig. 3a), an edge  $\overline{cd}$  moves to a new edge  $\overline{c'd'}$ . The orthogonal distance between the two edges ( $d_1$ ) is called the critical shrinkage distance (CSD). The accumulated CSD for generating a skeleton vertex  $V$  is called the shrinkage grade of the vertex, denoted by  $G(V)$ . See Fig. 3a, the shrinkage grade of  $e''$  is  $G(e'') = (d_1 + d_2)$ .

2.3 Deriving a ray-based complete skeleton

The algorithmic flow [10] for deriving the ray-based complete skeleton of a polygon is described below. Given a polygon, the CSD for a shrinkage cycle is computed first and is followed by the computing of the result of the shrinkage cycle. The dangling edges are then removed, and the residual polygonal areas, if they exist, are further shrunk in the next shrinkage cycle. The shrinkage cycles are performed repeatedly until no residual area exists for further shrinkage. Detailed procedures of the algorithm can be referred in [10].

2.4 Leaf-trimming and graft-trimming

The ray-based skeleton looks more complicated than the original polygon (Fig. 3b). The leaf-trimming method [10] removes the skeleton links that are the firing traces of all vertices on the original polygon. An example is shown in Fig. 3c, which is not exactly L-shaped. The graft-trimming process removes the skeleton links that are the firing traces of all vertices in each shrinkage cycle. Reducing the length of the removed link to zero would generate a skeleton that is exactly L-shaped (Fig. 3d). Yet, the graft-trimmed method may produce a null skeleton (empty set) for non-rectilinear polygons.

3 Area-trimming method

This section describes the area-trimming method for pruning the ray-based skeleton. Each skeleton link is interpreted as a modeling area inside the polygon. The criteria and the method for creating such a modeling area are first presented. Then we show that the union of the modeling areas of all skeleton links is identical to the original polygon. Finally, the definition of virtual links and the method used to identify virtual links are described.

3.1 Criteria for defining the modeling area

We propose four criteria for defining the modeling area of a skeleton link. Let  $P$  be a polygon,  $L$  be one of its skeleton links and  $A(L)$  be the modeling area of  $L$ .

Criterion 1: the area  $A(L)$ , if shrunk according to the ray-based propagation rules, would produce a skeleton involving  $L$ .

Criterion 2:  $A(L)$  is a polygon.

Criterion 3: each edge on  $A(L)$  should be relevant to (i.e., parallel to or collinear with) an edge of polygon  $P$ .

Criterion 4:  $A(L)$  should be a subset of polygon  $P$ .

3.2 Creating polygons for criteria 1 and 2

To meet criteria 1 and 2, we first define the reference area of a skeleton link, which is a region bounded by two lines and two circular arcs. The concept is illustrated by Fig. 4c, where  $\overline{V_1V_2}$  denotes a link of the ray-based skeleton where  $G(V_1) = r_1$  and  $G(V_2) = r_2$ . Let  $C_1$  and  $C_2$  be the two circles centered at  $V_1$  and  $V_2$  with radii  $r_1$  and  $r_2$ , respectively, and let  $L_1$  and  $L_2$  be the two lines tangent to both  $C_1$  and  $C_2$ . The region bounded by  $L_1, L_2, A_1$ , and  $A_2$  is the reference area of the skeleton link  $\overline{V_1V_2}$ , where  $A_1$  and  $A_2$  are the two circular arcs of  $C_1$  and  $C_2$  that are tangent to  $L_1$  and  $L_2$ .

Based on the reference area model, a polygon that meets criteria 1 and 2 can be derived in two steps. As Fig. 5a illustrates, we first identify any two points  $X_1$  and  $X_2$ , located respectively on arcs  $A_1$  and  $A_2$ . Next, two lines  $L_3$  and  $L_4$  are found, tangent to  $A_1$  and  $A_2$  at  $X_1$  and  $X_2$ , respectively. The polygon, say  $P_1$ , bounded by lines  $L_1, L_2, L_3$ , and  $L_4$  would satisfy criteria 1 and 2. Namely, if polygon  $P_1$  is shrunk according to the ray propagation model, the skeleton link  $\overline{V_1V_2}$  would be generated. This characteristic can easily be proved because  $V_1$  is equidistant from lines  $L_1, L_2$ , and  $L_3$ ;  $V_2$  is equidistant from lines  $L_1, L_2$ , and  $L_4$ .

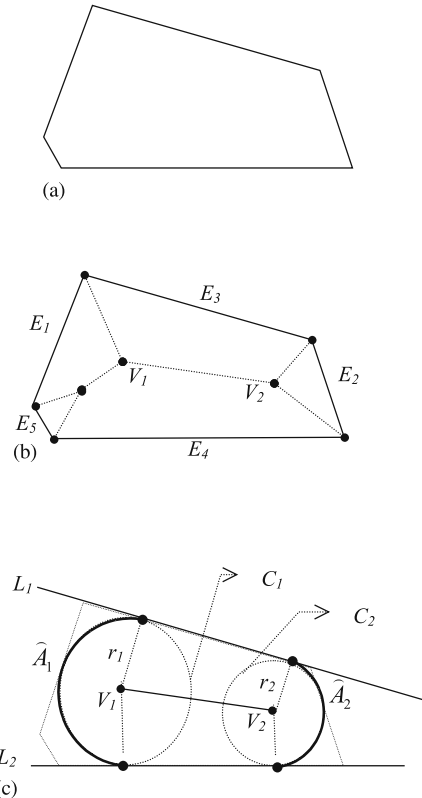


Fig. 4. a Original polygon. b Ray-based skeleton. c Reference area of a skeleton link

Notably, polygons satisfying criteria 1 and 2 are not unique. We can easily make such a polygon, say  $P_2$ , by adding two extra lines to  $P_1$ , namely  $L_5$  and  $L_6$ , which are respectively tangent to arc  $A_1$  and  $A_2$  at other points (Fig. 5b). The polygon  $P_2$  would also meet criteria 1 and 2 according to similar arguments to that for  $P_1$ .

### 3.3 Creating polygons for criteria 3 and 4

The lines bounding the polygon meeting criteria 1 and 2 can be classified into two sets: the tube line set and the cap line set. For the skeleton link  $V_1V_2$  in Fig. 5b, the set of lines  $\{L_1, L_2\}$ , tangent to both the two arcs  $A_1$  and  $A_2$ , is termed its tube line set. Meanwhile, the set of lines  $\{L_3, L_4, L_5, L_6\}$  tangent to either of the two arcs  $A_1$  and  $A_2$  is termed the cap line set of the skeleton link. Notice that each of the tube lines pass through an edge of the original polygon.

To meet criterion 3, the cap lines should be relevant to the polygon edges. One way to meet this criterion is by requesting the cap lines be collinear with the polygon edges tangent to arc  $A_1$  or arc  $A_2$ ; for example, line  $L_7$  and line  $L_8$  in Fig. 5c for the polygon in Fig. 4a. The polygon, say  $P_3$ , bounded by  $L_1, L_2, L_7$ , and  $L_8$ , also meets criteria 1 and 2. However, confining cap lines to all polygon edges tangent to  $A_1$  or  $A_2$  may not be sufficient, since the resulting polygon may be larger than the area bounded by the original polygon (Fig. 6a), or no such cap line exists (Fig. 6b).

To overcome these drawbacks, a cap line is proposed for each polygon edge that is not tangent to  $A_1$  or  $A_2$ . If a polygon edge is not tangent to any of the two arcs, the line collinear with the edge should be offset toward the interior of the polygon until it

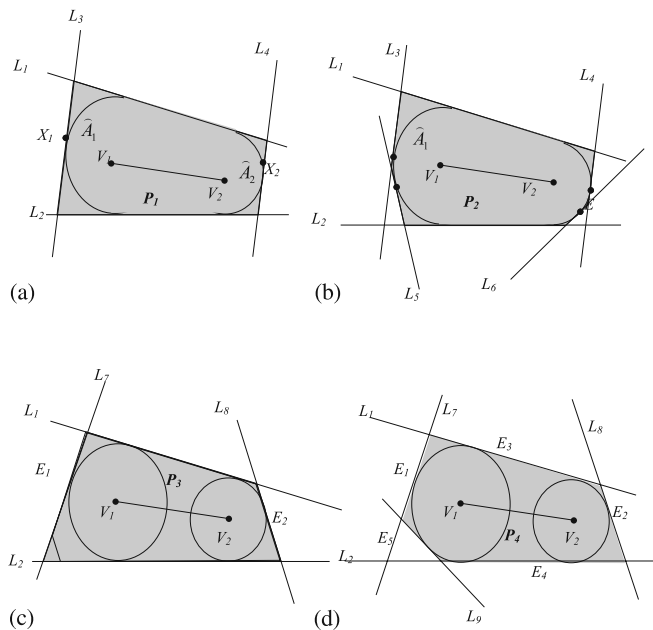
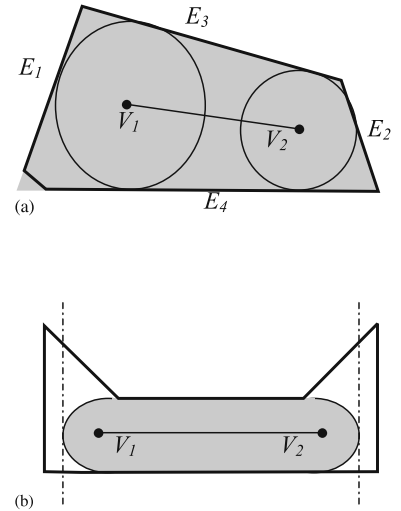


**Fig. 5a–d.** The process for deriving the modeling area of a skeleton link. **a** Polygon that meets both criteria 1 and 2. **b** Polygon that meets both criteria 1 and 2. **c** Polygon that meets criteria 1 and 2 may not meet criterion 3. **d** Polygon that meets criteria 1, 2, and 3

**Fig. 6a,b.** Two drawbacks of polygons that only meet criteria 1 and 2. **a** The polygon is larger than the original polygon. **b** Cap lines may not exist



is tangent to either  $A_1$  or  $A_2$ . As Fig. 5d and Fig. 4b show, line  $L_9$  is derived as the cap line of edge  $E_5$ . The polygon derived in this manner is termed the modeling area (M-area) of the skeleton link. The M-area of a skeleton link  $L$  is denoted by  $A(L)$ .

Given a polygon  $P = \{e_1, e_2, \dots, e_m\}$  – where  $e_i$  is a polygon edge – and its ray-based skeleton  $S = \{s_1, s_2, \dots, s_n\}$ , where  $s_k$  is a skeleton link, let the line passing through  $e_i$  be  $N_i$ , and the half-space divided by  $N_i$ , which includes the firing path of  $e_i$ , be  $H_i$ . The procedure for creating  $A(s_k)$  is summarized below.

- Step 1: for a skeleton link  $s_k$ , determine its two end-points ( $V_1$  and  $V_2$ ) and its shrinkage grades ( $r_1$  and  $r_2$ ).
- Step 2: determine the two circles ( $C_1$  and  $C_2$ ) centered at  $V_1$  and  $V_2$  with radii  $r_1$  and  $r_2$ .
- Step 3: determine tube lines  $L_{t1}$  and  $L_{t2}$  and the two circular arcs  $A_1$  and  $A_2$ .  $L_{ti}$  denotes a line tangent to both  $C_1$  and  $C_2$ , while  $A_i$  is an arc on  $C_i$  with its two end-points on  $L_{t1}$  and  $L_{t2}$ .
- Step 4: determine the cap lines.
  - For ( $i = 1$  to  $m$ )
  - /\*Determine the cap line  $L_{ci}$  with respect to  $s_k$  for each polygon edge  $e_i$ \*/
  - If  $N_i$  intersects  $s_k$ , then  $L_{ci} = null$
  - Else if  $s_k \not\subset H_i$ , then  $L_{ci} = null$
  - Else if  $N_i$  is tangent to either  $A_1$  or  $A_2$ , then  $L_{ci} = N_i$
  - Else
  - Offset  $N_i$  toward  $s_k$  until it is tangent to either  $C_1$  or  $C_2$ .
  - Let the offset of  $N_i$  be  $N'_i$ .
  - If  $N'_i$  is tangent to  $A_1$  or  $A_2$ , then  $L_{ci} = N'_i$
  - Else  $L_{ci} = null$
  - End
- Step 5: for  $L_{tj}$  ( $j = 1, 2$ ) and  $L_{ci}$ , determine the half spaces that contain  $s_k$  which are termed  $H_{ti}$  and  $H_{ci}$
- Step 6: determine the M-area of  $s_k$

$$A(s_k) = (\bigcap_j H_{tj}) \cap (\bigcap_i H_{ci})$$

Notice that the reference area of a skeleton link is inside the original polygon. For each polygon edge that tends to move toward the reference area, a cap line or a tube line is defined to enclose the reference area. The M-area thus formed is a convex polygon and would meet criterion 4, i.e.,  $A(L)$  is a subset of the original polygon or  $A(L) \subset P$ .

### 3.4 Union of M-areas of all skeleton links

The M-area of a skeleton link has one important characteristic. The union of the M-areas of all skeleton links is identical to the original polygon. Before explaining the rationale, two characteristics of the ray-based skeleton are introduced.

First, an edge on a polygon will shrink to a set of mutually connected line segments (termed the shrunk line segments), and the two end-points of the line segments are the two vertices of the edge. Furthermore, the region bounded by the edge and its shrunk line segments is a polygon. As shown in Fig. 7a,  $\overline{V_0V_4}$  is an edge of polygon  $P$ , and its shrunk line segments involve four mutually connected segments – namely,  $\overline{V_0V_1}$ ,  $\overline{V_1V_2}$ ,  $\overline{V_2V_3}$ ,  $\overline{V_3V_4}$  – while its two end vertices are  $V_0$  and  $V_4$ . The region bounded by edge  $\overline{V_0V_4}$  and its four shrunk line segments is a polygon denoted by  $S(\overline{V_0V_4})$  and indicates that the edge  $\overline{V_0V_4}$  would move over the shrunk region  $S(\overline{V_0V_4})$  thoroughly during ray propagation.

Second, a polygon can be decomposed into several sub-areas, each of which corresponds to the shrunk region of a polygon edge. Furthermore, the union of these sub-areas is identical to the ori-

ginal polygon. As illustrated in Fig. 7a, the polygon has been decomposed into five sub-areas  $S_i (1 \leq i \leq 5)$ , where  $S_i$  denotes the shrunk region of edge  $e_i$ . Once the resulting ray-based skeleton is produced, no more areas should exist for further shrinkage. This implies that the polygon has been thoroughly decomposed by the ray-based skeleton or polygon  $P = \cup_{j=1}^5 S_j$ . That is, each point in the interior of the polygon only belongs to a particular sub-area.

Let  $P$  be a polygon,  $\{e_j, j = 1, \dots, n\}$  be the edges of  $P$ ,  $\{L_i, i = 1, \dots, m\}$  be the skeleton link of  $P$ ,  $H(e_j)$  be the shrunk region of edge  $e_j$ , and  $S = \cup_{i=1}^m A(L_i)$  be the union of the modeling areas of all skeleton links. As stated, polygon  $P$  is completely decomposed by the shrunk regions,  $P = \cup_{j=1}^n H(e_j)$ . We can easily derive  $S \subset P$ , because  $A(L_i) \subset P$  for  $i = 1, \dots, m$ . If we can prove that  $P \subset S$ , then  $P = S$ .

To prove  $P \subset S$  or  $\{\cup_{j=1}^n H(e_j)\} \subset S$ , we merely have to show that the shrunk region of each edge is a subset of  $S$ , i.e.,  $H(e_j) \subset S$ . A shrunk region can be decomposed into several projection areas,  $H(e_j) = \cup_k PJ(L_k)$ , where  $PJ(L_k)$  denotes the projection area associated with skeleton link  $L_k$ . As shown in Fig. 7b,  $\overline{V_0V_n}$  is an edge on a polygon, and its shrunk line segments are  $\overline{V_0V_1}$ ,  $\overline{V_1V_2}, \dots, \overline{V_{n-1}V_n}$ . The orthogonal projection of  $V_i$  on edge  $\overline{V_0V_n}$  is designated as  $V'_i$ . For a skeleton link  $\overline{V_iV_{i+1}}$ , the area bounded by polygon  $V'_iV_iV_{i+1}V'_{i+1}$ , called the projection area of the skeleton link  $\overline{V_iV_{i+1}}$ , is a subset of the reference area of  $\overline{V_iV_{i+1}}$  and is a subset of its M-area (Fig. 7b). That is, each projection area of a skeleton link is a subset of its M-area; i.e.,  $PJ(L_k) \subset A(L_k)$ . This further implies that the shrunk region of each edge is a subset of  $S$ ; i.e.,  $H(e_j) = \{\cup PJ(L_k)\} \subset \{\cup A(L_k)\} = S$ . Therefore,  $P = \cup_j H(e_j) \subset S$ . Since  $P \subset S$  and  $S \subset P$ , we can derive  $P = S = \cup A(L_k)$ .

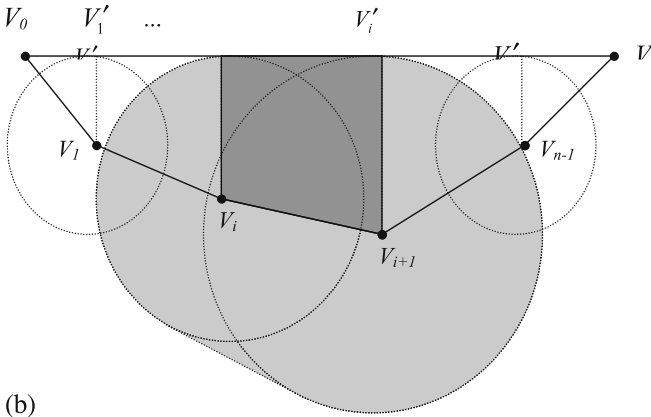
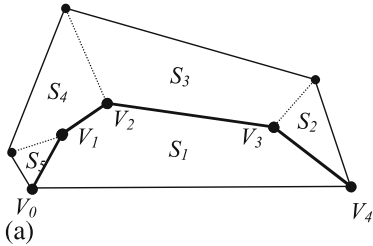


**Fig. 7a,b.** Union of all modeling areas is identical to the original polygon. **a** The modeling area is a subset of original polygon. **b** The original polygon is a subset of the union of all modeling areas

### 3.5 Virtual links

Each link of the ray-based skeleton has an M-area, and the union of the M-areas of all links is identical to the area bounded by the original polygon. However, some skeleton links may be redundant in terms of area modeling and are called virtual links. A skeleton link that is not a virtual link is termed a real link. A virtual link is defined as described below.

Let  $L$  be a link on a ray-based skeleton and  $L_i (i = 1, \dots, m)$  be the links neighboring  $L$ ; their M-areas are  $A(L)$  and  $A(L_i)$ . Link  $L$  is a virtual link if a neighboring link  $L_k$  exists such that  $A(L) \subset A(L_k)$  and  $A(L) \neq A(L_k)$ .

The procedure for deriving virtual links and real links is presented below. Let  $P$  be a polygon, while  $\{L_i, i = 1, \dots, m\}$  is the set of skeleton links of  $P$ , and  $A(L_i)$  is the modeling area of link  $L_i$ .

Step 1: let  $R = \{L_i, i = 1, \dots, m\}$  and  $V = \emptyset$

Step 2: for ( $i = 1$  to  $m$ )

{Identify the neighboring links of  $L_i$ .

Check if  $L_i$  is a virtual link.

If  $L_i$  is virtual link,  $V \leftarrow L_i, R = R - \{L_i\}$ .

Else

End}

Step 3: output  $R$  and  $V$ , where  $R$  denotes the set of real links and  $V$  represents the set of virtual links.

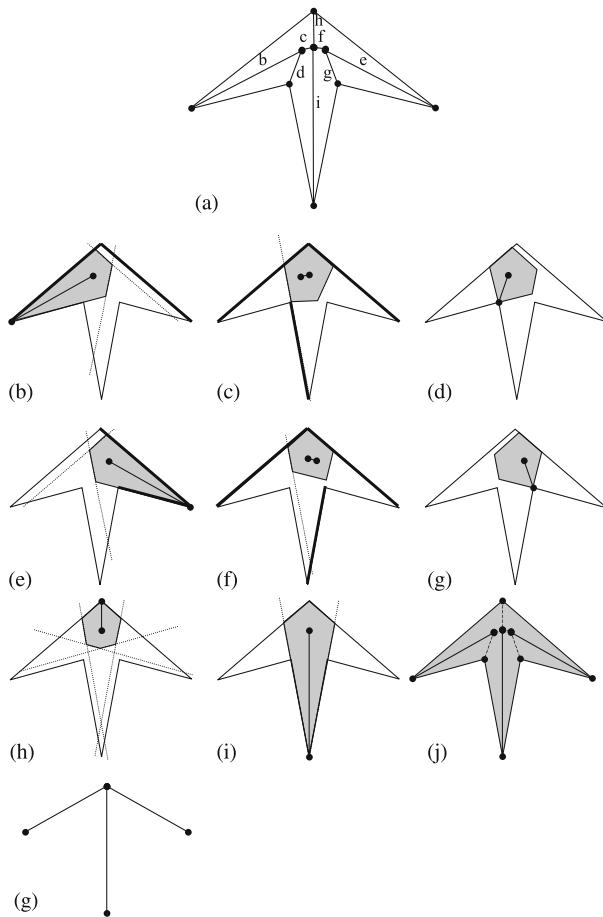


**Fig. 8a–k.** Modeling area of each skeleton link. **a** Polygon with skeleton. **b–i** Modeling area of link b-i. **j** Union of all modeling areas. **k** A-trimmed skeleton

The set of real links of a ray-based skeleton is termed the area-based trimmed skeleton (A-trimmed skeleton). The A-trimmed skeleton can be described by a tree structure that can be derived from the complete skeleton by reducing the length of virtual links to zero while maintaining their connections with its adjacent links. That is, virtual links are removed and their neighboring real links are joined together.

Figure 8 displays the M-areas of the eight skeleton links of a polygon. Following the procedure for identifying virtual links, the ray-based skeleton can finally be characterized as having three real links  $\{b, e, i\}$  and five virtual links  $\{c, d, f, g, h\}$ , since  $A(c) \subset A(i)$ ,  $A(f) \subset A(i)$ ,  $A(h) \subset A(i)$ ,  $A(d) \subset A(b)$ ,  $A(g) \subset A(e)$ . Figure 8k shows the resulting A-trimmed skeleton after removing virtual links. The union of the real links  $A(b) \cup A(e) \cup A(i)$  is identical to the area bounded by the original polygon.

## 4 Analysis and comparison

This section first analyzes the differences among the skeletons that are based on the ray propagation model. Then, possible modifications of the MAT, a wave-based skeleton, are justi-

fied. Finally, for some non-rectilinear polygons, the proposed A-trimmed skeletons are compared with other skeletons.

### 4.1 Ray-based skeletons

As stated above, derivation of the A-trimmed skeleton for a polygon involves two steps. The first step is to generate the ray-based complete skeleton by applying a grass-firing paradigm that uses the ray-based propagation model. The second step is to trim the ray-based complete skeleton based on an area-trimming methodology. The leaf-trimming skeleton [10], the graft-trimming skeleton [11], and the A-trimming skeleton proposed in this paper are all based on the ray-based fire propagation model. Each of the three skeletons is generated by pruning the ray-based complete skeletons, but are based on different trimming methods. The leaf-trimming method removes the skeleton link that is on the firing traces of all vertices on the original polygon. The graft-trimming method removes the skeleton links that is on the firing traces of all vertices in each shrinkage cycle. These two trimming methods are relatively heuristic and their applications to non-rectilinear polygons would generate skeletons not similar to the original polygons. The A-trimming method on the other hand is more systematic; it removes the skeleton links whose modeling areas tend to be redundant in characterizing the original polygon.

The A-trimmed skeleton in essence is an area decomposition approach. That is, the area of a polygon is decomposed into several areas and each area is modeled by a real skeleton link. Virtual links, on the other hand, denote the connecting relationships between real links. That is, they imply the neighboring relationships among the decomposed areas. Notice that the decomposed areas may mutually overlap.

### 4.2 Possible modification of the MAT

From the above discussion, the A-trimmed skeleton, as a global shape descriptor, seems better than the MAT. Readers may wonder whether the MAT could be improved by making some modifications. One possibility is to remove the “seam edges” [12] from the MAT. The seam edges are the skeleton links located on the bisector of two neighboring edges of the original polygon, and the resulting skeleton is called the trimmed-MAT. The trimmed-MAT by nature cannot eliminate the inclusion of curved segments due to the application of the wave-base propagation model. Another possibility for further improving the MAT is to replace the curved segment on the trimmed MAT by a line segment. This again cannot resolve the problem of being sensitive to small geometrical variations, as illustrated in Fig. 2.

The MAT, in fact, cannot be trimmed from the perspective of characterizing a polygon by area decomposition. Each skeleton link in both the ray-based complete skeleton and the MAT individually models an area. For the two types of skeletons, the union of the modeling areas of all links is identical to the original polygon. Some links in the ray-based skeleton are virtual and can be removed. Yet, each skeleton link in the MAT is a real link and cannot be removed.

According to the definition of the MAT, the modeling area of a point on a skeleton link is a disc that fits inside the object but is not a subset of any other maximum inscribed circle of the object. Consequently, for the MAT, each skeleton link is a real link; that is, no link can be removed in characterizing a polygon. Suppose one particular point on a skeleton link can be removed. Then its modeling area (a disc) must be a subset of some other discs; this is in conflict with the definition of the MAT. Therefore, each point on a skeleton link is indispensable from the perspective of area modeling. This feature implies that the MAT cannot be further simplified based on the concept of polygonal area decomposition.

One fundamental difference between the A-trimmed skeleton and the MAT is the fire propagation model. The fire propagates like a ray in the A-trimmed skeleton, yet propagates like a wave in the MAT. The ray propagation feature implies that each skeleton link of the A-trimmed skeleton is linear. That is, the linearity of polygons is preserved in the ray-based propagation model. In the wave-based propagation model, linearity cannot be preserved and certainly cannot be recovered by heuristically replacing the curved segments by line segments.

#### 4.3 Examples

This research has tested many examples for comparing the A-trimmed skeleton with others. Some of the examples are shown in Fig. 9, where the A-trimmed skeleton is compared with the ray-based skeleton, the leaf-trimmed skeleton, and the graft-trimmed skeleton. Notice that the inherent drawbacks of the MAT and the trimmed-MAT skeletons have been analyzed, as

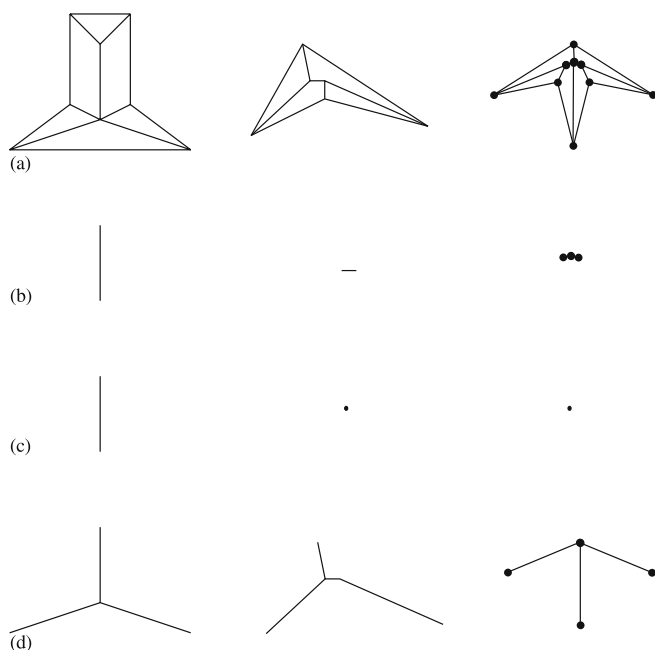


**Fig. 9a–d.** Comparison of various skeletons. **a** Polygon and ray-based skeleton. **b** The leaf-trimmed skeleton. **c** The graft-trimmed skeleton. **d** The A-trimmed skeleton, where ● denotes an empty set

illustrated in Fig. 2. From these examples, we can see that the A-trimmed skeleton is a better global shape descriptor than others in modeling a polygon.

## 5 Concluding remarks

This study presents a new global shape descriptor for a polygon, termed the area-trimmed (A-trimmed) skeleton. Derivation of the A-trimmed skeleton for a polygon involves two steps. The first step is to generate the ray-based complete skeleton by applying a grass-firing paradigm that uses the ray-based propagation model. The second step is to prune the ray-based complete skeleton based on an area-trimming method. The area-trimming method appears more logical than the trimming methods proposed in the literature [10, 11].

The A-trimmed skeleton also performs better in modeling polygons in the application of object classification than does the traditional definition of skeletons given by Blum in the 1960s [4], which has been used by most researchers during the past three decades. Likewise, the A-trimmed skeleton is also superior to the leaf-trimmed skeleton [10] and the graft-trimmed skeleton [11] in this application.

The following features distinguish the A-trimmed skeleton. First, the A-trimmed skeleton is structurally more concise than previous approaches, and does not include any curved segments. Second, the appearance of the A-trimmed skeleton closely resembles its polygon, since it was developed based on the idea of area decomposition. Third, the A-trimmed skeleton provides a novel concept that indicates virtual links in the skeleton are redundant in terms of area modeling. That is, when the modeling areas of virtual links are excluded, the union of the remaining modeling areas remains identical to the original polygon. The concept of virtual links provides a theoretical basis for explaining why the A-trimmed skeleton is inherently more concise than others, and more closely resembles the global shape of the original polygon.

The A-trimmed skeleton, like other global shape descriptors of polygons, can be applied to the automatic classification of prismatic parts [1] and punched parts [2]. Meanwhile, the clustered objects can be used to facilitate fixture [3] or part design by a “design-by-retrieval” paradigm.

**Acknowledgement** The Council in Taiwan is acknowledged for financially supporting this research under Contract No. NSC87-2212-E009-017.

## References

1. Wu MC, Jen SR (1996) A neural network approach to the classification of 3D prismatic parts. *Int J Adv Manuf Technol* 11:325–335
2. Cheok BT, Zhang YF, Leow LF (1997) A skeleton-retrieving approach for the recognition of punched parts. *Comput Ind* 32:249–259
3. Wu MC, Yen JY (1992) A skeleton-retrieving technique for aiding modular fixtures design. *Int J Adv Manuf Technol* 8:123–128
4. Blum H (1967) A transformation for extracting new descriptors of shape. In: Whalen-Dunn W (ed) *Models for the perception of speech and vision form*. MIT Press, Cambridge, pp 362–380

5. Blum H, Nagel RN (1978) Shape description using weighted symmetric axis features. *Patt Recogn* 10:167–180
6. Montanari, U (1968) A method for obtaining skeletons using a quasi-Euclidean distance. *J ACM* 15:600–624
7. Preparata FP (1977) The media axis of a simple polygon. In: *Proceeding of 6th Symposium on Mathematical Foundations of Computer Science*, pp 443–450
8. Lee DT (1982) Medial axis transformation of a planar shape. *IEEE Trans Patt Anal Mach Intell* 4:363–369
9. Bookstein FL (1979) The line-skeleton. *Comput Graph Image Process* 11:1223–1237
10. Wu MC, Chen JR (1994) A skeleton approach to modeling 2D workpieces. *J Des Manuf* 4:229–243
11. Wu MC, Chen JR, Jen SR (1994) Global shape information modeling and classification of 2D workpieces. *Int J Comput Integr Manuf* 7:261–275
12. Sherbrooke EC, Patrikalakis NM, Brisson E (1995) Computation of the medial axis transform of 3-D polyhedra. *IEEE Trans Vis Comput Graph* 2:62–72